

Growth and Characterization of Large-size InSe Crystal from Non-stoichiometric Solution *via* a Zone Melting Method

JIN Min¹, MA Yupeng², WEI Tianran², LIN Siqi¹, BAI Xudong³, SHI Xun⁴, LIU Xuechao⁴

(1. School of Materials Science, Shanghai Dianji University, Shanghai 201306, China; 2. School of Materials Science and Engineering, Shanghai Jiao Tong University, Shanghai 200240, China; 3. Wuzhen Laboratory, Tongxiang 314500, China; 4. Shanghai Institute of Ceramics, Chinese Academy of Sciences, Shanghai 200050, China)

Abstract: Indium selenide (InSe) is a III-VI group semiconductor with interesting physical properties and has wide potential applications in the fields of photovoltaics, optics, thermoelectrics, and so on. However, the production of large-size InSe crystal is difficult due to the inconsistent melting of In and Se elements and peritectic reactions between InSe, In₆Se₇ and In₄Se₃ phases. In this work, a zone melting method, which has advantages of low cost and solid-liquid interface optimization, is employed for InSe crystal preparation. Because the initial mole ratio of In to Se is of great importance to InSe crystal growth, the non-stoichiometric In_{0.52}Se_{0.48} solution was precisely used for growth based on the peritectic reaction of In-Se system, resulting in a InSe crystal productivity ratio at about 83%. An ingot with dimensions $\phi 27$ mm \times 130 mm is obtained with a typical slab-like InSe crystal in the size of $\phi 27$ mm \times 50 mm. The successfully peeled cleavage plane exhibits the good single-crystalline character as only (00 l) peaks are detected in the X-ray diffraction pattern. This crystal has a hexagonal structure, and its elements are distributed uniformly in the matrix with transmittance of $\sim 55.1\%$ at 1800 nm wavelength, band gap energy of about 1.22 eV, a maximum electrical conductivity (σ) of about 1.55×10^2 S \cdot m⁻¹ along the (001) direction, and a lowest thermal conductivity (κ) of about 0.48 W \cdot m⁻¹ \cdot K⁻¹ perpendicular to the (001) direction at 800 K. These results imply that the zone melting method is indeed an effective approach for fabricating large-size InSe crystal, which could be applied for various fields. Above measured electrical and thermal behaviors are expected to provide a significant reference for InSe crystal application in the future.

Key words: InSe crystal; zone melting method; non-stoichiometric; electrical conductivity; thermal conductivity

InSe is an interesting layer-structured III-VI group semiconductor with a moderately direct band gap, high electron mobility, and pronounced photoluminescent response, thus showing diverse potential applications in the fields of photovoltaics, optics, thermoelectrics, and so on^[1-9]. For example, Han *et al.*^[1] reported InSe as one of the most promising materials with absolute advantages in field-effect transistors (FETs) due to its high electron mobility and stable material properties. Cao *et al.*^[2] announced hBN-encapsulated atomically thin InSe allowed high-quality optics and electron transport

devices. Yu *et al.*^[3] found that multilayer InSe-based diode showed a high forward rectification ratio over 10^3 without gate-modulation at room temperature, which was superior to most multilayer van der Waals heterojunctions (vdWHs) devices. Cui *et al.*^[4] revealed that InSe doped with Sn achieved a thermoelectric figure of merit $ZT = 0.23$ at 830 K by increasing the carrier concentration from $\sim 10^{14}$ cm⁻³ to $\sim 10^{15}$ cm⁻³, highlighting its potential as a thermoelectric material. Recently, it is reported that single-crystalline InSe exhibits a remarkable plastic deformability that is rarely observed

Received date: 2023-11-09 **Revised date:** 2023-12-28; **Published online:** 2024-03-19

Foundation item: National Natural Science Foundation of China (52272006, 52371193, 52001231); Shanghai Academic/Technology Research Leader (23XD1421200); Oriental Scholars of Shanghai Universities (TP2022122); Space Application System of China Manned Space Program, Shanghai Rising-star Program (23QA1403900); Chengguang Program supported by Shanghai Education Development Foundation & Shanghai Municipal Education Commission; Open Research Fund of Key Laboratory of Polar Materials and Devices, Ministry of Education

Biography: JIN Min (1982–), male, professor. E-mail: jmaish@aliyun.com

金 敏(1982–), 男, 教授. E-mail: jmaish@aliyun.com

Corresponding author: LIU Xuechao, professor. E-mail: xcliu@mail.sic.ac.cn
刘学超, 研究员. E-mail: xcliu@mail.sic.ac.cn

in inorganic semiconductors, offering a new avenue towards flexible/hetero-shaped electronic devices^[10-12]. Therefore, it is convinced that the research on InSe semiconductor will develop fast in the future.

Large-size crystal is essential to studying the structure and properties of InSe semiconductors. On the one hand, it can reflect the nearly intrinsic structures, defects, and properties. On the other hand, the big crystal is an important raw material to prepare mono- or few layer materials by *e.g.*, mechanical exfoliation. However, it should be noted that the preparation of large-size InSe crystal is difficult due to the inconsistent melting of In and Se elements and the peritectic reactions between InSe/In₆Se₇/In₄Se₃ according to the In-Se phase diagram^[5]. Up to now, a lot of approaches have been developed to produce InSe crystals, such as the Czochralski method, horizontal gradient freeze method, low temperature liquid phase method, vapor transfer method, vertical Bridgman method, and so on^[6]. However, it remains a persistent challenge to produce large or high-quality InSe crystals. For instance, Chevy *et al.*^[13] ever produced InSe crystal from the stoichiometric solution by using the Czochralski method, but many parasitic nucleations appeared on the (001) faces of the crystal. Tang *et al.*^[14] explored a low temperature liquid phase method using InSe_{0.77} solution and Se gas source as raw materials, resulting in the inclusion of a significant amount of In elements in the crystals. Medvedeva *et al.*^[15] reported that the InSe crystal produced *via* the vapor transfer method was only 0.3 mm×0.3 mm×0.1 mm in size and some In₆Se₇ phases were embodied. In recent years, the vertical Bridgman method was considered a feasible way for bulk InSe crystals preparation. As an example, a ϕ 14 mm×40 mm boule with large area InSe crystal was successfully obtained from a stoichiometric melt^[16]. Moreover, a ϕ 25 mm×75 mm ingot was also fabricated from the In_{0.52}Se_{0.48} non-stoichiometric solution in our previous work^[10], which displayed a high mole percentage of InSe crystal due to the peritectic reaction in the melt. Frankly speaking, in order to meet the rapidly growing demand for academic research and applications, the development of novel methods for large-size InSe crystal growth remains an urgent challenge.

In this work, a zone melting method is introduced for InSe crystal preparation. Compared to the traditional vertical Bridgman method, this technique has obvious advantages of low cost and solid-liquid interface optimization during crystallization, which has been successfully employed for many kinds of semiconductor crystals fabrication in the past, such as GaAs, SnSe, Mg₃Sb₂, ZnTe, and so on^[17-20]. Ultimately, a boule with dimensions of ϕ 27 mm×130 mm is produced, and a pile of large area slab-like InSe crystals are smoothly peeled

from the ingot along the cleavage plane. Furthermore, the crystal structure, optical, electrical and thermal properties are also characterized. The obtained results indicate that the zone melting method is indeed an effective way for large-size InSe crystal growth which can be used for research and applications in the future.

1 Experimental

1.1 InSe crystal preparation

High-purity In and Se elements (>99.99%) with the mole ratio of 0.52 : 0.48 were used as start materials and the total weight was about 342.48 g. Fig. 1(a) shows the dependence of weight percentage of In and Se on temperature measured by thermogravimetry equipment (TG-DTA 8121, Japan). It is found the weight of In kept stable in the range of 300–1000 K. However, there is a significant loss of Se beginning at 620 K, and it is completely exhausted near 790 K. Based on this knowledge, a rocking method is introduced for polycrystal synthesis. The In and Se elements were loaded into a ϕ 27 mm quartz ampoule that was sealed with $<10^{-3}$ Pa vacuum and then placed into a 1020 K rocking furnace. After the start materials were melted and soaked for 10 min, the furnace was worked at a rate of 30 r/min for half an hour to promote the reaction sufficiently. Then, the furnace was cooled to room temperature naturally. InSe crystal growth was carried out by a homemade zone melting furnace, as the schematic diagram described in Fig. 1(b). A quartz crucible containing the prepared In_{0.52}Se_{0.48} polycrystal was placed into the furnace and supported by an Al₂O₃ block. A pair of Pt/Pt-10%Rh thermocouples were installed near the bottom of quartz crucible for temperature indication. The furnace temperature was controlled at \sim 970 K, a sufficiently high temperature for InSe crystal preparation. After the polycrystal was melted and soaked for 10 h, InSe crystal growth was gradually executed at a rate of 0.6 mm/h under a temperature gradient of \sim 30 K/cm. Finally, the furnace was cooled to room temperature at a rate of 40–50 K/h.

1.2 Characterization

The crystal density (ρ) was measured *via* the Archimedes principle. The phase structure was analyzed by X-ray diffractometer (Bruker D8, Germany) using Cu K α radiation ($\lambda=0.15406$ nm) at room temperature. The crystal composition was measured by energy dispersive spectrometer (Oxford Instruments, Britain). The transmittance was examined by ultraviolet visible near infrared spectrophotometer (LAMBDA, China). The crystal dislocations were revealed by using the acid solution (30 g K₂Cr₂O₇, 50 mL concentrated H₂SO₄ and

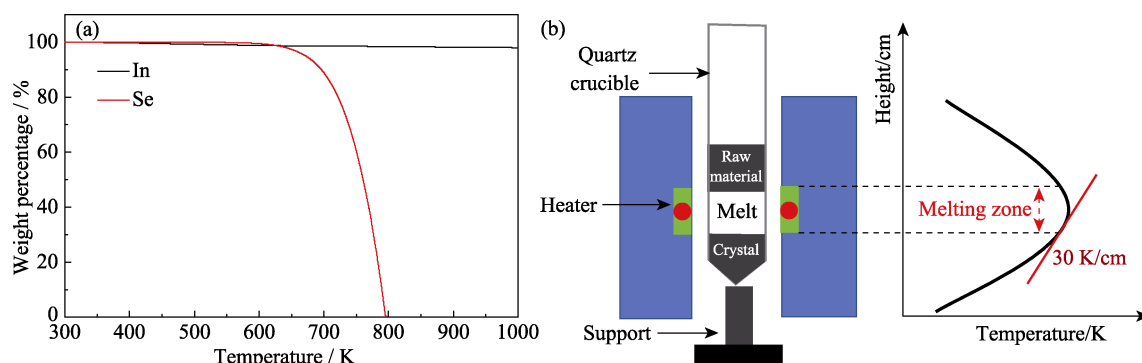


Fig. 1 Crystal growth design

(a) Dependence of weight percentage of In/Se elements on temperature; (b) Schematic diagram of zone melting method for InSe crystal growth

300 mL distilled water), and then observed by normal optical microscope (FLY-L3230, China) and white light confocal microscope (ZEISS Smart Proof 5, Germany). The electrical conductivity was tested by thermoelectric measurement equipment (ULVAC-RIKO, ZEM-3) from room temperature to 800 K, and the thermal diffusivity (D) was characterized through a laser flash method (Netzsch, LFA-457, Germany) over 300–800 K.

2 Results and discussion

According to the In-Se phase diagram in Fig. 2, the inconsistent melting of In and Se elements and the peritectic reactions between InSe/ In_6Se_7 / In_4Se_3 make the initial mole ratio crucial for obtaining pure phased InSe single crystals. In detail, if In and Se elements are weighted according to their standard stoichiometric ratio, In_6Se_7 will firstly crystallize near 630 °C (as the red dotted line indicated), followed by the production of InSe when the temperature is lowered to ~600 °C, where a peritectic reaction occurs between In_6Se_7 and the solution. However, when the non-stoichiometric melt $\text{In}_{0.52}\text{Se}_{0.48}$ is cooled to ~600 °C, InSe will firstly form and part of them will transfer to In_4Se_3 through another peritectic reaction at around 550 °C (as the blue dotted line indicated). It should be noted that the window passage for

InSe fabrication from non-stoichiometric solution is much narrow. Chevy *et al.*^[13] reported the upper limit of Se was 45.0% (in atomic) and the lower limit was only 34.4% (in atomic). Nevertheless, Imai *et al.*^[21] modified the In-Se phase diagram depending on the careful composition design and differential thermal analysis (DTA). Ultimately, the window passage was adjusted to 38.0%–48.3% (in atomic). Therefore, a non-stoichiometric $\text{In}_{0.52}\text{Se}_{0.48}$ solution, rather than stoichiometric InSe, provides a more feasible and effective way to grow large-sized InSe crystal.

The narrow high temperature zone of the furnace is much valuable for InSe crystal preparation. As previous literature reported, InSe crystal has a low thermal conductivity compared to those of GaAs, InSb, GaSb, *etc.*^[17, 22-24]. Therefore, it is anticipated that a large amount of crystallization latent heat will accumulate near the solid-liquid interface during the crystal growth, leading to a concave interface that might introduce kinds of defects in the crystal, such as inclusions, twinning, heavy dislocations, parasitic nucleations, *etc.*^[25-26]. Fortunately, the narrow temperature zone is beneficial for solid-liquid interface optimization as the latent heat can be conducted along both up and down directions simultaneously.

Fig. 3(a) exhibits the as-grown ingot just taken out from the quartz ampoule. It is about $\phi 27 \text{ mm} \times 130 \text{ mm}$ in dimensions, the largest size so far. Table 1 lists the growth results of InSe crystals by different methods in the past years. The ingot can be divided into two parts according to the peritectic reaction principle. The powder XRD patterns from middle and top parts of the ingot are indexed to be hexagonal InSe (PDF#34-1431) and In_4Se_3 (PDF#51-0808) phases, respectively, as shown in Fig. 3(b). In addition, some In elements (PDF#05-0642) are detected in the In_4Se_3 matrix because the crystal grows from an In-rich solution. Such residual In phase is a common problem that also happened in the vertical Bridgman method using the same $\text{In}_{0.52}\text{Se}_{0.48}$

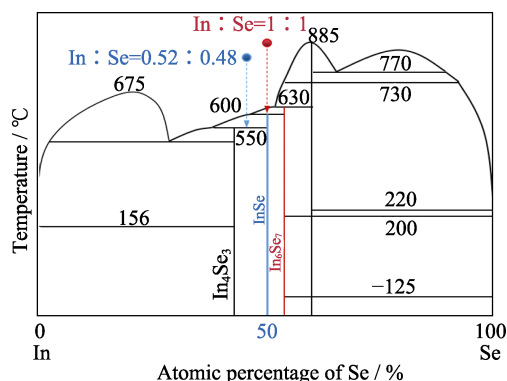


Fig. 2 In-Se binary phase diagram

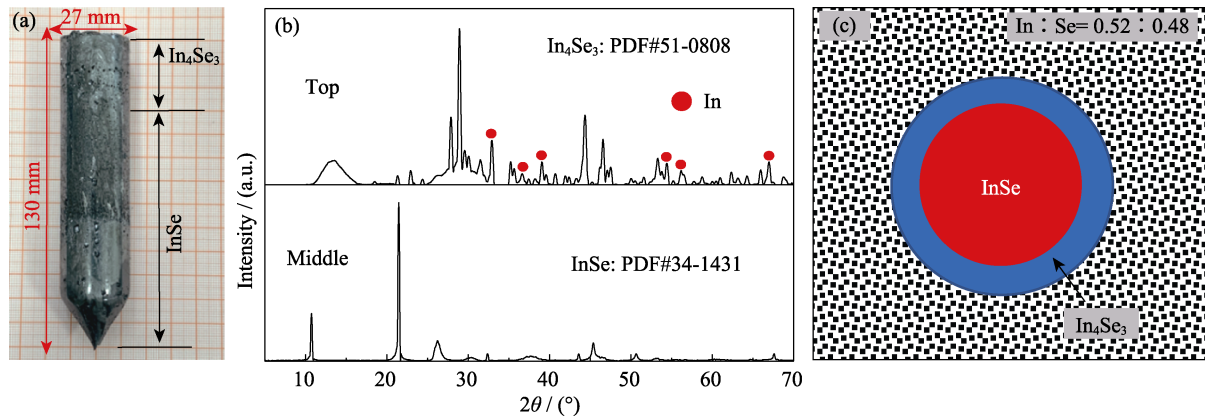


Fig. 3 Results of as-grown ingot

(a) Photo of as-grown ingot; (b) Powder XRD patterns of the middle and top parts of the ingot; (c) Transfer relationship between InSe and In₄Se₃ phases

Table 1 Growth results of InSe crystals by different methods in the past years

Author	Year	Country	Method	$n(\text{In}) : n(\text{Se})$	Crystal size	Ref.
Damon R W <i>et al.</i>	1954	USA	Stockbarger	1 : 1	$\phi 10 \text{ mm} \times 20 \text{ mm}$	[28]
Andriyashik M V <i>et al.</i>	1968	Ukraine	Czochralski	1 : 1	$\phi 20 \text{ mm} \times (40-50) \text{ mm}$	[29]
Chevy A <i>et al.</i>	1977	France	Vertical Bridgman	0.56 : 0.44	$\phi 14 \text{ mm} \times 30 \text{ mm}$	[30]
Chevy A <i>et al.</i>	1978	France	Czochralski	0.56 : 0.44	$1 \text{ mm} \times 25 \text{ mm} \times 65 \text{ mm}$	[13]
Chevy A	1981	France	Chemical transport	1 : 1	$0.3 \text{ mm} \times 0.3 \text{ mm} \times 0.1 \text{ mm}$	[31]
Imai K <i>et al.</i>	1981	Japan	Vertical Bridgman	0.52 : 0.48	$\phi 10 \text{ mm} \times 50 \text{ mm}$	[21]
Blasi C D <i>et al.</i>	1982	Italy	Vertical Bridgman	0.52 : 0.48	$\phi 10 \text{ mm}$	[32]
Chevy A	1984	France	Modified Bridgman	0.56 : 0.44	$\phi 10 \text{ mm}$	[33]
Tribloullet R <i>et al.</i>	1986	France	Travelling heater	0.52 : 0.48	$\phi 15 \text{ mm} \times 60 \text{ mm}$	[34]
Ishii T	1988	Japan	Vertical Bridgman	0.52 : 0.48	$\phi 10 \text{ mm}$	[27]
Gurbulak B	1999	Turkey	Freezing method	1 : 1	$\phi 12 \text{ mm} \times 60 \text{ mm}$	[35]
Icelli O <i>et al.</i>	2004	Turkey	Stockbarger	1 : 1	$\phi 12 \text{ mm} \times 60 \text{ mm}$	[36]
Gurbulak B <i>et al.</i>	2014	Turkey	Bridgman-Stockbarger	1 : 1	$\phi 10 \text{ mm} \times 60 \text{ mm}$	[37]
Wei T R <i>et al.</i>	2020	China	Vertical Bridgman	0.52 : 0.48	$\phi 25 \text{ mm} \times 75 \text{ mm}$	[10]
Zhang B <i>et al.</i>	2021	China	Vertical Bridgman	1 : 1	$\phi 14 \text{ mm} \times 40 \text{ mm}$	[16]
Shi H <i>et al.</i>	2021	China	Vertical Bridgman	1 : 1	$\phi 12.7 \text{ mm} \times 12 \text{ mm}$	[24]
Jin M <i>et al.</i>	2023	China	Zone melting method	0.52 : 0.48	$\phi 27 \text{ mm} \times 130 \text{ mm}$	This work

compound as raw material^[27]. Fig. 3(c) illustrates the transfer relationship between InSe and In₄Se₃ phases during crystal growth. When In_{0.52}Se_{0.48} solution is moved from high temperature zone to the temperature gradient zone, InSe phase would firstly crystallize, then the In₄Se₃ phase will gradually grow up through the reaction between InSe and the In-rich solution. The final mole percentage of InSe in the whole ingot is calculated to be ~83% according to the following formula^[21]:

$$\frac{M_{\text{InSe}}}{M_{\text{Ingot}}} = \frac{C_0 - C_p}{C_{\text{InSe}} - C_p} \quad (1)$$

Where M_{InSe} is the InSe weight, M_{Ingot} is the ingot weight, $C_0 = 48\%$ is the initial Se content, $C_{\text{InSe}} = 50\%$ is the mole percentage of Se in InSe, and $C_p = 38\%$ is the lower limit of Se among the window passage range.

InSe is a layered structure material: the monolayer is composed of Se-In-In-Se atomic planes through strong covalent/ionic bonds while the layers are connected via the weak van der Waals interactions. Therefore, InSe crystal can be readily exfoliated. A pile of slab-like InSe crystals are smoothly peeled from the ingot along the cleavage plane. Fig. 4(a) is a typical specimen with an area of about $\phi 27 \text{ mm} \times 50 \text{ mm}$. Fig. 4(b) exhibits the slab has good single-crystalline character as only (00 $\bar{1}$) peaks are detected in the XRD pattern examined on the cleavage plane. Here, attention should be paid to the wrinkled crystal surfaces and its step configurations, which are mainly attributed to the soft mechanical property and layered structure of InSe when they are manually processed. Fig. 4(c) shows a piece of mirror-like InSe wafer and a fresh flake is disclosed by

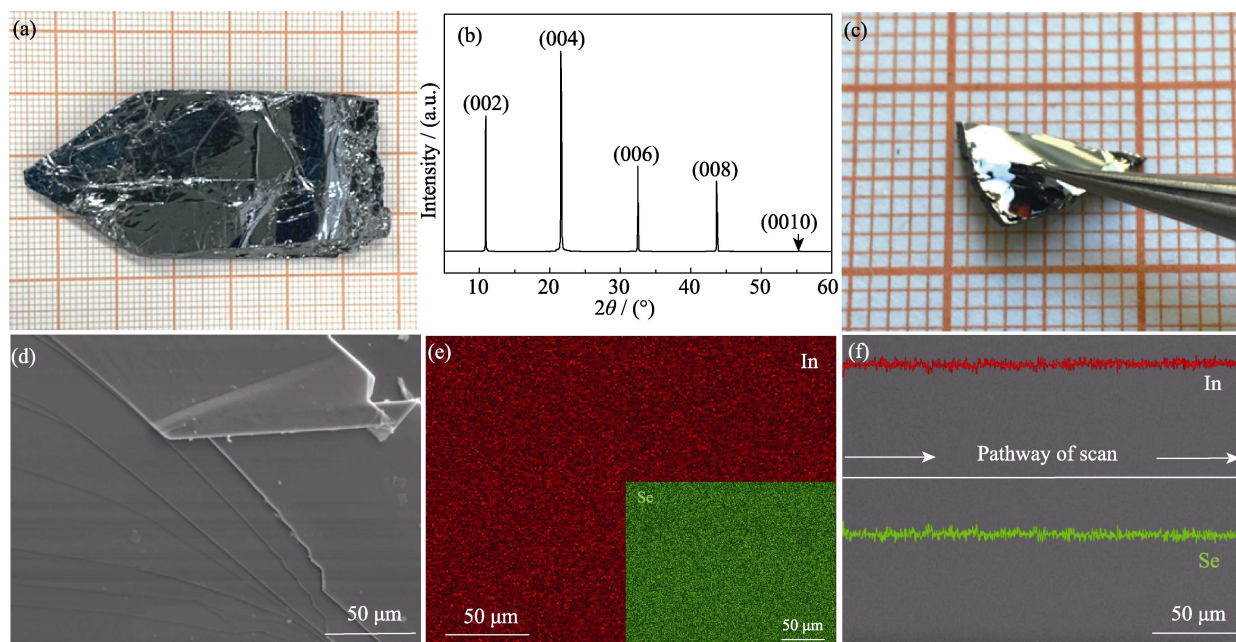


Fig. 4 Characterization of obtained single crystals

(a) Large area slab-like InSe crystal cleaved from the ingot; (b) XRD pattern of (001) cleavage plane; (c) Fresh flake disclosed by tweezers; (d) SEM image of (001) plane; (e) Area scan and (f) line scan by EDS

tweezers. The new exposed surface is analyzed by SEM and the layered morphology is clearly observed in Fig. 4(d). Fig. 4(e) shows the EDS mappings reveal In and Se elements are uniformly distributed in the matrix. The EDS line scan diagram in Fig. 4(f) further verifies the crystal has a high composition homogeneity. Based on these results, it is convinced the zone melting method is indeed a competitive technique for large-size InSe crystal fabrication.

The transmittance spectrum of a 0.8 mm thickness (001) wafer is given in Fig. 5(a). It is totally opaque below 1020 nm relates to its absorption edge. However, as the wavelength is gradually increased to 1060 nm, the transmittance (T) undergoes a sharp increase. After that, the growth of T is gentle and ultimately reaches the highest of 55.1% at 1800 nm. This result means InSe crystal has nice near infrared transmittance. Based on this transmittance spectrum, the band gap energy E_g of InSe can be deduced by Equation (2)^[18]:

$$(ah\nu)^2 = C(h\nu - E_g) \quad (2)$$

Here h is the Planck's constant, ν is the frequency of incident photon, C is a constant for direct transition, and α is the absorption coefficient can be gained by:

$$\alpha = (1/d)\ln(100/T) \quad (3)$$

Where d is the wafer thickness and T is the transmittance. Finally, the dependence of $(ah\nu)^2$ on $h\nu$ is drawn in Fig. 5(b) and E_g is deduced to be ~ 1.22 eV that agrees well with the previous studies^[15, 23].

Fig. 6(a) shows the relationship of electrical conductivity (σ) with temperature along (001) plane. It is noted here

that the σ is not detected below 450 K which implies the InSe crystal has high resistance near room temperature. The σ is kept on a low level before 600 K, and the smallest value is about $0.58 \text{ S} \cdot \text{m}^{-1}$ at 450 K. However, as temperature surpasses 600 K, the σ suddenly rises and finally reaches a biggest value of $1.55 \times 10^2 \text{ S} \cdot \text{m}^{-1}$ at 800 K. Such electrical conductivity variation tendency is mainly attributed to the intrinsic semiconducting transport behavior of InSe. As for the thermal transport behavior, the thermal diffusion D perpendicular to (001) plane is studied, as shown in Fig. 6(b). When temperature is increased from 300 K to 800 K, the D is reduced more than half from $0.79 \text{ mm}^2/\text{s}$ to $0.33 \text{ mm}^2/\text{s}$. However, as temperature is back to 300 K, the D returns to $0.72 \text{ mm}^2/\text{s}$ that implies InSe has good thermal diffusion reversibility. Based on the D , the thermal conductivity κ can be obtained by Equation (4)^[37]:

$$\kappa = \frac{3NRD\rho}{M} \quad (4)$$

Where N is the number of atoms in InSe molecular formula, R is the molar gas constant, $\rho = 5.568 \text{ g/mm}^3$ is the measured density and M is molecular weight of InSe. Obviously, the temperature- κ curve would display a similar shape compared with that of thermal diffusion. The average κ at 300 K is about $1.08 \text{ W} \cdot \text{m}^{-1} \cdot \text{K}^{-1}$ and the lowest value is $0.48 \text{ W} \cdot \text{m}^{-1} \cdot \text{K}^{-1}$ at 800 K which is consistent with the other reported results^[23]. InSe is a typical van der Waals layer-structured semiconductor and is easy to cleave along the in-plane direction, leading to difficulty in obtaining flake along the out-of-plane

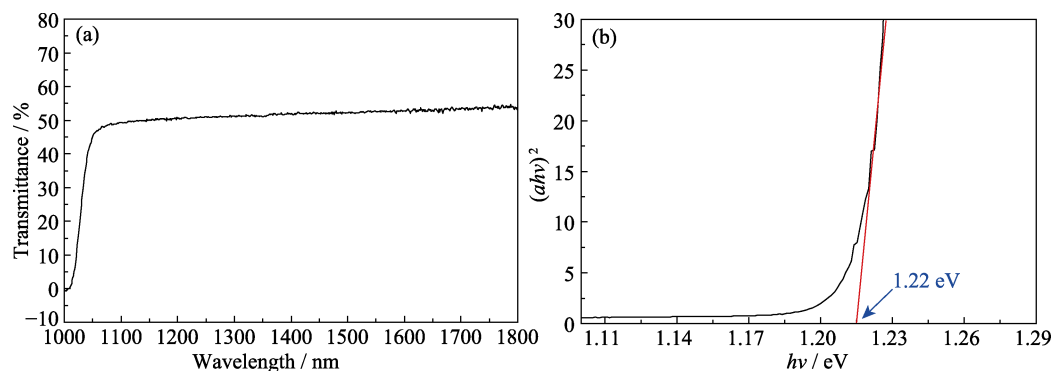


Fig. 5 Optical characterizations of InSe crystal

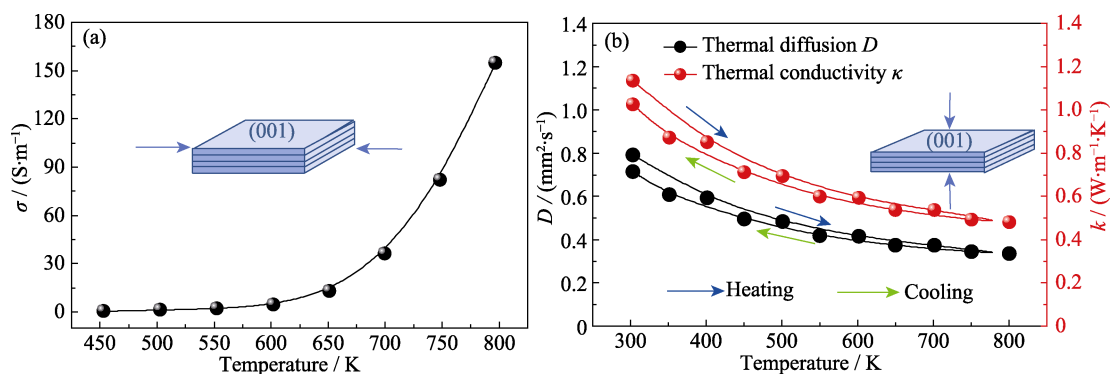
(a) Transmittance spectrum; (b) Band gap energy E_g 

Fig. 6 Transport properties under different temperatures

(a) Electrical conductivity σ ; (b) Thermal diffusion D and thermal conductivity κ

Colorful figures are available on website

directions. To the best of our knowledge, the in-plane thermal conductivity for bulk InSe is not available so far, and this remains to be addressed in the future. The measured electrical and thermal behaviors in this work provide significant reference for InSe crystal application.

3 Conclusions

In summary, a $\phi 27$ mm \times 130 mm InSe crystal has been successfully prepared using a zone melting method from non-stoichiometric $\text{In}_{0.52}\text{Se}_{0.48}$ solution based on the peritectic reaction of In-Se system. The productivity ratio of InSe crystal is about 83%. The as-grown InSe crystal shows a layered crystal structure and the In/Se elements are uniformly distributed. The band gap energy is determined as ~ 1.22 eV via the transmittance spectrum. The crystal has a highest electrical conductivity of $1.55 \times 10^2 \text{ S}\cdot\text{m}^{-1}$ along (001) and a lowest thermal conductivity of $0.48 \text{ W}\cdot\text{m}^{-1}\cdot\text{K}^{-1}$ perpendicular to (001) near 800 K.

References:

- [1] JIANG J F, LI J X, LI Y T, *et al.* Stable InSe transistors with high-field effect mobility for reliable nerve signal sensing. *npj 2D Mater. Appl.*, 2019, **3**(1): 29.
- [2] BANDURIN D A, TYURNINA A V, YU G L, *et al.* High electron mobility, quantum Hall effect and anomalous optical response in atomically thin InSe. *Nat. Nanotechnol.*, 2016, **12**(3): 223.
- [3] YU M M, HU Y X, GAO F, *et al.* High-performance devices based on InSe- $\text{In}_{1-x}\text{Ga}_x\text{Se}$ van der Waals heterojunctions. *ACS Appl. Mater. Interf.*, 2020, **12**(22): 24978.
- [4] HOU X J, CHEN S P, DU Z L, *et al.* Improvement of the thermoelectric performance of InSe-based alloys doped with Sn. *RSC Adv.*, 2015, **5**(124): 102856.
- [5] HE F, BAI X D, LU X Y, *et al.* Research progress of III-VI group InSe semiconductor crystal growth. *J. Synth. Cryst.*, 2022, **51**(9/10): 1722.
- [6] ZHAO Q H, ZHENG D, CHEN P, *et al.* Research progress on indium selenide crystals and optoelectronic devices. *J. Synth. Cryst.*, 2022, **51**(9/10): 1704.
- [7] GUO Z, CAO R, WANG H, *et al.* High-performance polarization-sensitive photodetectors on two-dimensional beta-InSe. *Natl. Sci. Rev.*, 2022, **9**(5): nwab098.
- [8] PASQUALE G, LOPRIORE E, SUN Z, *et al.* Electrical detection of the flat-band dispersion in van der Waals field-effect structures. *Nat. Nanotechnol.*, 2023, **18**(12): 1416.
- [9] SUI F, JIN M, ZHANG Y, *et al.* Sliding ferroelectricity in van der Waals layered gamma-InSe semiconductor. *Nat. Commun.*, 2023, **14**: 36.
- [10] WEI T R, JIN M, WANG Y, *et al.* Exceptional plasticity in the bulk single-crystalline van der Waals semiconductor InSe. *Science*, 2020, **369**(6503): 542..
- [11] HAN X. Ductile van der Waals materials. *Science*, 2020, **369**(6503): 509.
- [12] MA Y P, HUANG H R, LIU Y F, *et al.* Remarkable plasticity and softness of polymorphic InSe van der Waals crystals. *J. Materiomics*, 2023, **9**: 709.
- [13] CHEVY A, GOUSKOV A, BESSON J M. Growth of crystalline

- slabs of layered InSe by the Czochralski method. *J. Cryst. Growth*, 1978, **43(6)**: 756.
- [14] TANG C, SATO Y, TANABE T, *et al.* Low temperature liquid phase growth of crystalline InSe grown by the temperature difference method under controlled vapor pressure. *J. Cryst. Growth*, 2018, **495**: 54.
- [15] MEDVEDEVA Z S, GULIEV T N. Growing single crystals of the indium selenide from the gas phase. *Inorg. Mater.*, 1965, **1(6)**: 848.
- [16] ZHANG B, WU H, PENG K L, *et al.* Super deformability and thermoelectricity of bulk γ -InSe single crystals. *Chin. Phys. B*, 2021, **30(7)**: 078101.
- [17] JIN M, SHEN H, FAN S J, *et al.* Industrial growth and characterization of Si-doped GaAs crystal by a novel multi-crucible Bridgman method. *Cryst. Res. Technol.*, 2017, **52(6)**: 1700052.
- [18] JIN M, LIN S Q, LI W, *et al.* Nearly isotropic transport properties in anisotropically structured n-type single-crystalline Mg_3Sb_2 . *Mater. Today Phys.*, 2021, **21**: 100508.
- [19] JIN M, YANG W H, WANG X H, *et al.* Growth and characterization of ZnTe single crystal via a novel Te flux vertical Bridgman method. *Rare Met.*, 2020, **40(4)**: 858.
- [20] JIN M, TANG Z Q, ZHANG R L, *et al.* Growth of large size SnSe crystal via directional solidification and evaluation of its properties. *J. Alloys Compd.*, 2020, **824**: 153869.
- [21] IMAI K, SUZUKI K, HAGA T, *et al.* Phase diagram of In-Se system and crystal growth of indium monoselenide. *J. Cryst. Growth*, 1981, **54(3)**: 501.
- [22] JIN M, BAI X D, TANG Z Q, *et al.* Fabrication of InSb crystal via horizontal Bridgman method and investigation on its thermoelectric properties. *Mater. Res. Bull.*, 2021, **142**: 111411.
- [23] JIN M, TANG Z Q, ZHANG R L, *et al.* Growth of GaSb crystal and evaluation of its thermoelectric properties along (111) plane. *Cryst. Res. Technol.*, 2019, **55(1)**: 1900156.
- [24] SHI H, WANG D, XIAO Y, *et al.* Dynamic carrier transports and low thermal conductivity in n-type layered InSe thermoelectrics. *Aggregate*, 2021, **2(4)**: e92.
- [25] WANG W Y, CHEN X L, NI D Q, *et al.* Growth of near stoichiometric LiNbO_3 crystals by a modified zone melting method. *J. Alloys Compd.*, 2005, **402(1/2)**: 224.
- [26] LIU Y, AI F, PAN X H, *et al.* Effects of rotating magnetic field on $\text{Bi}_{12}\text{SiO}_{20}$ crystal growth by vertical zone-melting technique. *J. Cryst. Growth*, 2010, **312(9)**: 1622.
- [27] ISHII T. High quality single crystal growth of layered InSe semiconductor by Bridgman technique. *J. Cryst. Growth*, 1988, **89(4)**: 459.
- [28] DAMON R W, REDINGTON R W. Electrical and optical properties of indium selenide. *Phys. Rev.*, 1954, **96(6)**: 1498.
- [29] ANDRIYASHIK M V, SAKHNOVSKII M Y, TIMOFEEV V B, *et al.* Optical transitions in the spectra of the fundamental absorption and reflection of InSe single crystals. *Phys. Stat. Sol. (B)*, 1968, **28(1)**: 277.
- [30] CHEVY A, KUHN A, MARTIN M S. Large InSe monocrystals grown from a non-stoichiometric melt. *J. Cryst. Growth*, 1977, **38(1)**: 118.
- [31] CHEVY A. Growth of indium selenides by vapour phase chemical transport; polytypism of indium monoselenide. *J. Cryst. Growth*, 1981, **51(2)**: 157.
- [32] BLASI C D, MICOCCI G, MONGELLI S, *et al.* Large InSe single crystals grown from stoichiometric and non-stoichiometric melts. *J. Cryst. Growth*, 1982, **57(3)**: 482.
- [33] CHEVY A. Improvement of growth parameters for Bridgman-grown InSe crystals. *J. Cryst. Growth*, 1984, **67(1)**: 119.
- [34] TRIBLOULET R, CLEMENT C L, THEYS B, *et al.* Growth of InSe single crystals by the travelling heater method. *J. Cryst. Growth*, 1986, **79(1/2/3)**: 984.
- [35] GURBULAK B. Growth and optical properties of Dy doped and undoped n-type InSe single crystal. *Solid State Commun.*, 1999, **109(10)**: 665.
- [36] İCELLI Q, ERZENEGLU S, GURBULAK B. Mass attenuation coefficients for n-type InSe, InSe:Gd, InSe:Ho and InSe:Er single crystals. *J. Quant. Spectrosc. Radiat. Transf.*, 2004, **90(3/4)**: 399.
- [37] GURBULAK B, ŞATA M, DOĞAN S, *et al.* Structural characterizations and optical properties of InSe and InSe:Ag semiconductors grown by Bridgman/Stockbarger technique. *Physica E*, 2014, **64**: 106.

非化学计量溶液区熔法生长大尺寸 InSe 晶体及表征

金 敏¹, 马玉鹏², 魏天然², 林思琪¹, 白旭东³, 史 迅⁴, 刘学超⁴

(1. 上海电机学院 材料学院, 上海 201306; 2. 上海交通大学 材料科学与工程学院, 上海 200240; 3. 乌镇实验室, 桐乡 314500; 4. 中国科学院 上海硅酸盐研究所, 上海 200050)

摘 要: 硒化铟(InSe)是一种具有奇异物理性能的 III-VI 族半导体材料, 在光伏、光学、热电等领域有着广泛的应用潜力。由于 InSe 的非一致熔融特性及 InSe、 In_6Se_7 和 In_4Se_3 之间复杂的包晶反应, 制备大尺寸 InSe 晶体十分困难。本研究采用区熔法制备了 InSe 晶体, 该方法具有成本低、固液界面优化等优点。基于 In-Se 体系的包晶反应, 发现 In 与 Se 的初始物质的量比对 InSe 晶体生长非常重要, 本工作使用精确非化学计量的 $\text{In}_{0.52}\text{Se}_{0.48}$ 溶液生长晶体, 使 InSe 晶体的获得率达到 83% 左右。实验最终获得了 $\phi 27\text{ mm} \times 130\text{ mm}$ 的晶棒, 并成功剥离出尺寸 $\phi 27\text{ mm} \times 50\text{ mm}$ 的片状 InSe 单晶, XRD 图谱中检测到(001)衍射峰, 说明晶体的质量良好。InSe 晶体呈现六方结构, 各元素在基体中均匀分布, 在 1800 nm 波长下的透射率为~55.1%, 带隙能量为~1.22 eV。在 800 K 下, InSe 晶体沿(001)方向的最大电导率 σ 约为 $1.55 \times 10^2\text{ S} \cdot \text{m}^{-1}$, 垂直于(001)方向的最低热导率 κ 约为 $0.48\text{ W} \cdot \text{m}^{-1} \cdot \text{K}^{-1}$ 。上述结果表明, 区熔法是制备大尺寸 InSe 晶体的一种有效方法, 可用于制备多类材料。该工作制备的 InSe 的电学和热学行为也为今后 InSe 晶体的应用提供了重要参考。

关 键 词: InSe 晶体; 区熔法; 非化学计量; 电导率; 热导率

中图分类号: TQ174 文献标志码: A 文章编号: 1000-324X(2024)05-0554-07